Active Micro Motor Bearing

Ronald Mueller, Hannes Bleuler, Ueli Schlaepfer, Mathijs van der Meer

Institut de Microtechnique,
Swiss Federal Institute of Technology (EPFL)
1015 Lausanne, Switzerland
Fax No.: (+41 21) 693 38 66
E-Mail: ronald.mueller@imt.dmt.epfl.ch

Abstract: For motions in the micro-world mechanical friction and wear severely limit performance and lifetime. For linear and oscillatory motion, flexure hinges help to overcome this limitation, they are successfully implemented for e.g. linear accelerometers or precision instrumentation.

In the case of full rotation at high speed, contact-free support is one of the most promising solutions. Potential applications include gyroscopes, optical choppers, disc-drives for data storage and optical scanning for various instruments. Common to all these applications is the requirement of high precision of the rotor position. Therefore purely passive means of levitation such as e.g. paramagnetism, Meissner-Ochsenfeld, flux-pinning, AC bearings, will not suffice. Such systems will often need position sensing and active motion control.

These facts motivate the further development of active micro bearings. The first steps in this direction were presented in earlier papers [1]. Here we report on the continuation of these efforts. The main result reported is the contact free suspension and rotation of a rotor of sub-mm dimensions with active bearings.

1. Introduction

The active micro motor magnetic bearing which has been developed allows active control of three degrees of freedom (DOF). Only two DOF, the position of the rotor in the stator plane, have to be controlled with a feedback control system. Rotation can be achieved by feedforward control and the three DOF necessary for the contact free suspension of the rotor in the stator are stable without active control.

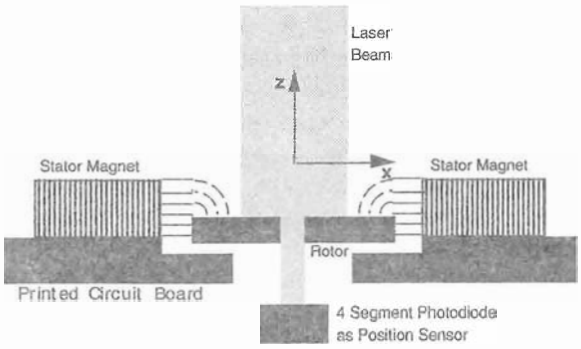

Fig. 1 Cut through the bearing: the rotor is actively controlled in x-y direction, in z direction it is stable because of reluctance forces.

Contact free levitation and rotation are achieved with the same coils. The motor is based on the principle of a reluctance motor. Two different control signals, one for the positioning and one for the drive of the motor, are superposed. The driving torque is created by modifying the bias currents in the radially opposed poles of the stator. The rotor has an octagonal shape and is surrounded by six independently controlled stator poles. The basic design principles for stepping / reluctance motors can be applied for the design.
Thus, no additional coils were necessary for the integration of the reluctance motor into the active magnetic bearing (AMB) system.

2. Configuration of the System

Laser cutting was applied for the production of rotor and stator. The limited precision obtainable with this manufacturing technique influenced the total design and the performances of the active micro motor bearing (AMMB). In a later step, the most critical part of the system, the rotor precision, was improved by the application of electro discharge machinery for its production. The rotor has a diameter of 950 µm and a thickness of 350 µm. The stator is 500 µm thick.
After the laser cutting, the stator was fixed on a standard board as used for printed circuits and covered by an isolating resine. The two parallel 22 turns for each of the six coils of the magnets were handwound and the completed system mounted on a conventional chip carrier. The diameter of the copper wire is 0.3 mm.

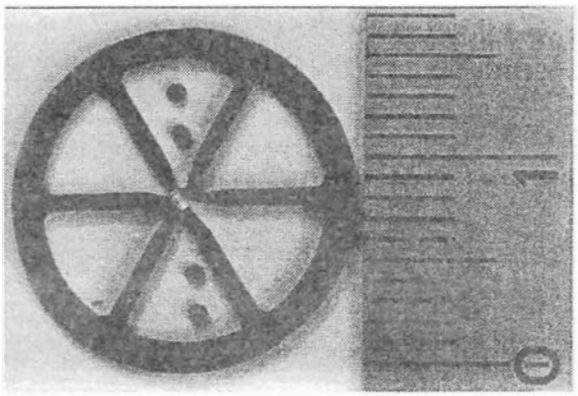

Fig. 2 A stator with six poles and four rotors (scale in cm)

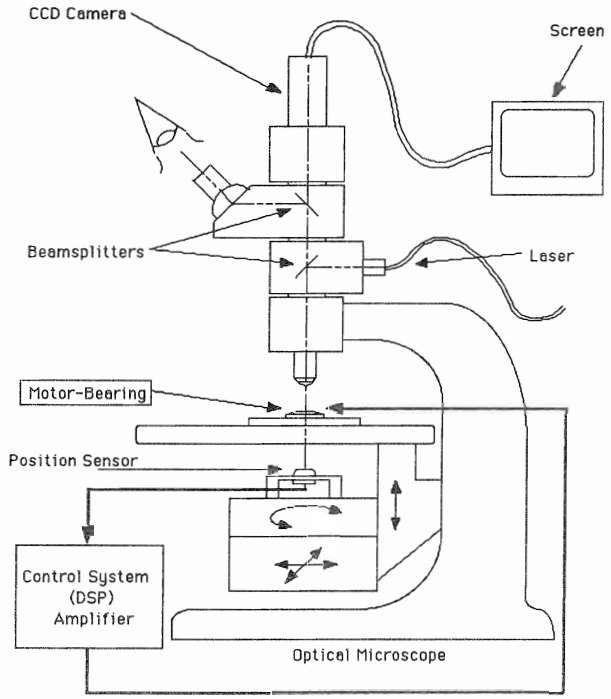

Fig. 3 Scheme of experimental setup

Fig. 4 Laboratory setup: the AMMB is mounted on the positioning table of an optical microscope.

For the experiment, the AMMB was placed under an optical microscope. The laser necessary for the position detection is injected into the optical path of the microscope by optical beamsplitters. Positioning tables allow the precise positionning of the AMMB and the four segment photodiode position sensor under the microscope.
A multichannel digital controller based on a C40 DSP is used to control the system. This allows a fairly easy implementation of different controller structures and online identification. The powersupply of the electromagnets is done with an analog amplifier with internal current feedback control.

3. Position Sensor

When miniaturizing an AMB, the choice of the position sensor necessary for the control loop is most essential. On one hand, the sensor has to have a very high resolution and large bandwith, on the other hand, the sensor should not exceed a certain size and provide the possibility of integration into the complete system.
In this system, an optical position sensor based on a laser source and a four segment photodiode was used. This sensors combines a very large bandwith with a high resolution. For some applications, e.g. Atomic Force Microscopy (AFM), resolutions up to 10 nm have been reported under stable operating conditions.
Other sensor principles such as integrated inductive sensors or capacitive sensors are under investigation.
The principle of this optical position sensor is based on the following figure:

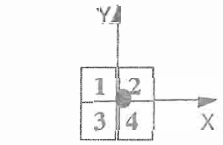

● : Laser Spot on
Four Segment Photodiode

Sensor Output :

$$U_x = (U_2 + U_4) - (U_1 + U_3)$$
$$U_y = (U_1 + U_2) - (U_3 + U_4)$$

Fig. 5 Calculation of the position with a 4 segment photodiode

3.1. Experimental Performances of the Position Sensor

During non operation of the bearing, the rotor was displaced relatively to the photodiode with the help of a x-y positionning table. A set of 9×9 equidistant measurement points with 50 measurements at each point were taken. The distance from point to point is 0.01 mm. The following figures show the average of the 50 measurements for each of the 9×9 equidistant measurement points.

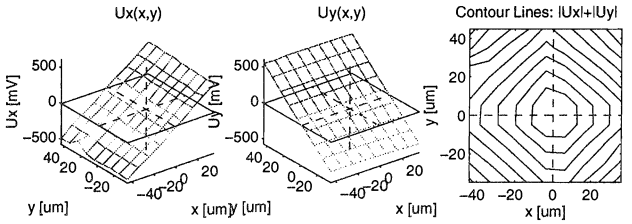

Fig. 6 Experimental position sensor performance

As the Fig. 6 shows, the sensor has an excellent linearity. The two position coodinates are well decoupled. A linear regression results in the following numerical equations.

$$\begin{pmatrix} U_x \\ U_y \end{pmatrix} = \begin{pmatrix} 11.5 & 0.724 \\ -0.140 & 12.24 \end{pmatrix} \cdot \begin{pmatrix} x \\ y \end{pmatrix} \qquad [\text{mV};\ \mu\text{m}]$$

The crosstalk between x and y is mainly result of a slight rotation of the photodiode in relation to the x-y table while the steepness depends on the current /voltage converter electronics.

4. Control and Performances

4.1. Digital Control

The system is controlled by two independent digital PD controllers in x-y-direction. The control of the position is based on PD controllers which create the controller output on the base of an error in the input. The control parameters remain constant.

The experimental results show a very robust behaviour to variations of the airgap which means that precise positionning of the rotor over a large range is possible.

The controllers were designed on Matlab/Simulink™ and crosscompiled to a C40 DSP. A realtime interface based on a dSPACE™ system was available.

4.1.1 Sampling Time

Due to the rather high eigenfrequency (800 Hz) of the AMMB system, the sampling time of the DSP system was chosen as short as possible. Without A/D and D/A conversion and data transfer to the host PC, the calculation time for the system on the DSP was about 70 microseconds.

$$\boxed{\begin{aligned} T_s &= 80 \quad [\mu\text{s}] \\ f_s &= 12.5 \quad [\text{kHz}] \end{aligned}}$$

Bearing design parameters such as bias current and the initial airgap as well as the mass of the rotor directly influence the eigenfrequency and thus have to be considered when using digital control.

4.2. Open Loop Transfer Function

As the AMMB system is instable without active control, the transfer function was measured in closed loop. The transfer function includes the power amlifier and the sensor dynamics. The measurement was done entirely in frequency domain. Because of the additional calculations during the measurement, the sampling time had to be raised up to 90 µs.

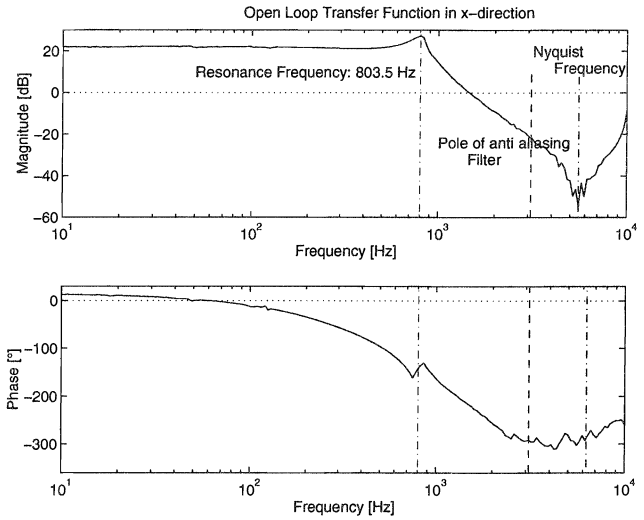

Fig. 7 Open loop transfer function in x-direction

4.2.1 Current Distribution on Coils

Variations of the inductance in the different coils were measured. The controller output gains were adjusted to these values.

4.2.2 Generation of the Rotating Magnetic Field

For the generation of a rotating magnetic field to drive the three phases of the reluctance motor, sinusoidal currents with a phase shift of 120° are applied to the poles.

The amplitude of the currents (65-80 mA) is relatively high compared to the bias current (180 mA). This has a strong influence on the stiffness of the system and has led to instability. In order to reduce this effect, a compensation is introduced: half of the current added to one pair of coils is substacted from each of the remaining two pairs of coils. Thus, the flux and the stiffness is increased in the direction of the rotating magnetic field while it is lowered in the perpendicular direction. Stability was obtained in this way.

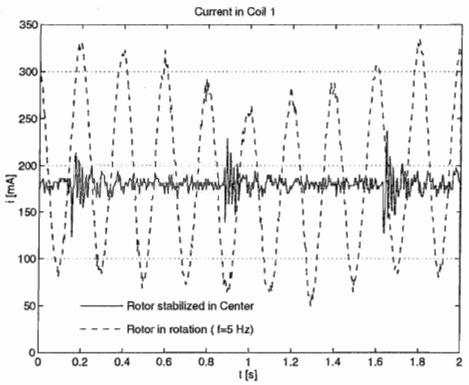

Fig. 8 Current in one coil of the bearing during standstill and rotation

Figure 8 shows the current measured in the coil during standstill (solid line) and rotation (dashed line). The perturbations visible on the solid curve are created by hitting the support table of the bearing and show the impulse response of the controller.

An interesting observation is the modulation of the current of the rotating magnetic field with a low frequency. This is the result of the excentricity of the rotor caused by the tolerances due to the manufacturing techniques (laser cutting). The field turns 60° and the rotor is aligned on the next pole which corresponds to a rotation of 15°.

A relatively strong compensation is required from the controller to keep the rotor in the center. The introduction of a PID controller could decrease this effect.

A continous variation of the rotational frequency in realtime can be performed.

Two nonlinear blocks for the calculation of sine and cosine are introduced. The third sine is calculated by the theorem of addition. This method was used in order to save calculation time.

4.3. Startup of the AMB using acoustic position feedback for the controller adjustment.

After a first, rough stabilization of the AMB system with a PD controller, the control parameters were acoustically fine-tuned. This was done by putting the position signals on an audio amplifier. As the human ear has the characteristics of an FFT analyzer and works up to frequencies of about 20 kHz, this method proved to be very convenient to tune the controller similary to the tuning of a musical instrument. Additionally, the position of the rotor in the *x*-*y*-plane was displayed on an oscilloscope to visualize the movements.

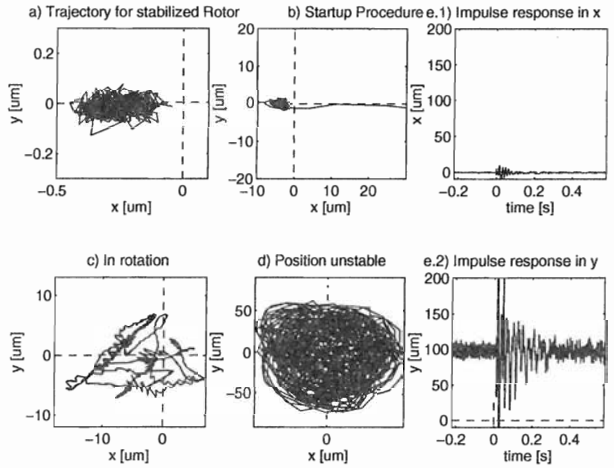

Fig. 9 Movement of the rotor under different operating conditions

a)This graph shows the position of the rotor during a period of one second. The rotor is well stabilized and the largest residual movements are in the order of 500 nm.

b)Here, the startup procedure of the rotor is shown. Before the activation of the controller, the rotor was in touchdown position on one side of the stator.

c)The lateral displacement of the rotor is clearly visible during the operation as motor bearing. The controller has to compensate the excentricity of the rotor due to the manufacturing tolerances. The graph shows a time capture of 2.5 seconds. The magnetic field turns at 10 Hz.

d) P controller without derivative term. The total lateral displacement can thus be visualized.

e)These two graphs show the movements of the rotor during a shock on the support table.

5. Conclusions and Outlook

In a relatively simple and standard setup, contact free rotation of a sub-mm rotor has been achieved. The machining of the rotor is not very precise. Yet sub-µm positionning precision at standstill and about 10 µm positionning precision during rotation have been achieved. Operation in all positions relative to gravity is possible. This opens up potential applications for very high rotational speed such as optical scanning, gyroscopes, data storage or others.

References

[1] H.Bleuler et al.: Micromachined Active Magnetic bearings, 4th International Symposium on Magnetic Bearings, Zurich, 1994